Earth and Planetary Science Letters 481 (2018) 80–90

Contents lists available at ScienceDirect

Earth and Planetary Science Letters

www.elsevier.com/locate/epsl

Age of Izu–Bonin–Mariana arc basement

Osamu Ishizuka [a,b,*], Rosemary Hickey-Vargas [c], Richard J. Arculus [d], Gene M. Yogodzinski [e], Ivan P. Savov [f], Yuki Kusano [a], Anders McCarthy [g,1], Philipp A. Brandl [h], Masafumi Sudo [i]

[a] Institute of Earthquake and Volcano Geology, Geological Survey of Japan, AIST, Central 7, 1-1-1, Higashi, Tsukuba, Ibaraki, 305-8567, Japan
[b] Japan Agency for Marine-Earth Science and Technology, 2-15 Natsushima, Yokosuka, Kanagawa, 237-0061, Japan
[c] Earth and Environment Department, Florida International University, Modesto Maidique Campus, AHC5-394, Miami, FL, 33199, USA
[d] Research School of Earth Sciences, The Australian National University, 142 Mills Road, Acton, ACT, 2601, Australia
[e] School of Earth, Ocean, and Environment, University of South Carolina, 701 Sumter Street, EWSC617, Columbia, SC, 29208, USA
[f] School of Earth and Environment, The University of Leeds, Institute of Geophysics and Tectonics, Leeds, LS2 9JT, UK
[g] Institute of Earth Sciences, University of Lausanne, Geopolis, Lausanne, 1015, Switzerland
[h] GEOMAR Helmholtz Centre for Ocean Research Kiel, Wischhofstr. 1-3, 24148, Kiel, Germany
[i] Institut für Erd- und Umweltwissenschaften, Universität Potsdam, Karl-Liebknecht-Str. 24, Haus 27, 14476, Golm, Germany

ARTICLE INFO

Article history:
Received 23 June 2017
Received in revised form 2 October 2017
Accepted 8 October 2017
Available online xxxx
Editor: A. Yin

Keywords:
subduction initiation
Izu–Bonin–Mariana arc
arc basement
$^{40}Ar/^{39}Ar$ age

ABSTRACT

Documenting the early tectonic and magmatic evolution of the Izu–Bonin–Mariana (IBM) arc system in the Western Pacific is critical for understanding the process and cause of subduction initiation along the current convergent margin between the Pacific and Philippine Sea plates. Forearc igneous sections provide firm evidence for seafloor spreading at the time of subduction initiation (52 Ma) and production of "forearc basalt". Ocean floor drilling (International Ocean Discovery Program Expedition 351) recovered basement-forming, low-Ti tholeiitic basalt crust formed shortly after subduction initiation but distal from the convergent margin (nominally reararc) of the future IBM arc (Amami Sankaku Basin: ASB). Radiometric dating of this basement gives an age range (49.3–46.8 Ma with a weighted average of 48.7 Ma) that overlaps that of basalt in the present-day IBM forearc, but up to 3.3 m.y. younger than the onset of forearc basalt activity. Similarity in age range and geochemical character between the reararc and forearc basalts implies that the ocean crust newly formed by seafloor spreading during subduction initiation extends from fore- to reararc of the present-day IBM arc. Given the age difference between the oldest forearc basalt and the ASB crust, asymmetric spreading caused by ridge migration might have taken place. This scenario for the formation of the ASB implies that the Mesozoic remnant arc terrane of the Daito Ridges comprised the overriding plate at subduction initiation. The juxtaposition of a relatively buoyant remnant arc terrane adjacent to an oceanic plate was more favourable for subduction initiation than would have been the case if both downgoing and overriding plates had been oceanic.

1. Introduction

Among the proposed hypotheses for the fundamentally important process of subduction zone initiation, two seem most widely relevant (e.g., Stern, 2004; Gerya, 2011): spontaneous initiation (e.g., Matsumoto and Tomoda, 1983; Stern and Bloomer, 1992; Stern, 2004; Nikolaeva et al., 2010), and induced (or forced) initiation (e.g., McKenzie, 1977; Gurnis et al., 2004; Maffione et al., 2015). Induced initiation may be triggered by externally forced compression, for example, along a pre-existing discontinuity, such as a fracture zone. Spontaneous subduction initiation occurs when a change in plate motion allows the gravitationally unstable lithosphere to subside and be subducted. Stern (2004) suggested the Izu–Bonin–Mariana arc (IBM arc) in the Western Pacific represents an example of spontaneous subduction initiation wherein subsidence of relatively old and dense Pacific lithosphere commenced along transform faults/fracture zones bounded by relatively buoyant lithosphere. Thorough reconstruction of the plates involved is required for testing the competing hypotheses for process of subduction initiation. Constraining the nature and origin of the

* Corresponding author at: Institute of Earthquake and Volcano Geology, Geological Survey of Japan, AIST, Central 7, 1-1-1, Higashi, Tsukuba, Ibaraki, 305-8567, Japan.
E-mail address: o-ishizuka@aist.go.jp (O. Ishizuka).
[1] Now at School of Earth Sciences, University of Bristol, Wills Memorial Building, Queens Road, Clifton, BS8 1RJ, UK.

https://doi.org/10.1016/j.epsl.2017.10.023
0012-821X/

overriding and subducting plates is especially important, because numerical modelling shows plate density is a key parameter controlling subduction initiation (e.g., Leng and Gurnis, 2015).

The IBM arc is an optimal place to investigate processes of subduction initiation. Extensive exposures of volcanic as well as plutonic lower crust and upper mantle sections in the present-day IBM forearc give access to a magmatic record preserved in the juvenile arc developed immediately after subduction initiation (e.g., Taylor et al., 1994; Ishizuka et al., 2006, 2011a, 2014a; Reagan et al., 2008, 2010, 2013). Disturbance of the exposed crustal section after its formation is minimal given the absence of overprinting by younger volcanism and significant tectonic movement. Erosion due to subduction of the Pacific Plate sustains exposure of the forearc section. The freshness of exposed samples allows most primary geochemical characteristics of the earliest magmatism to be characterised. Reliable age determination has provided a framework for constraining the temporal variation of magmatism associated with the development of subduction initiation and the formation of a subduction zone (Ishizuka et al., 2006, 2011a, 2014a; Reagan et al., 2008, 2010, 2013; Brounce et al., 2015).

Geochronology of igneous rocks from the IBM forearc section has revealed that the first basaltic magmatism (termed "forearc basalt" by Reagan et al., 2010) subsequent to subduction initiation was produced by decompression melting of highly-depleted mantle and commenced at 51–52 Ma (Ishizuka et al., 2011a; Reagan et al., 2013). Occurrence of sheeted dykes indicates that seafloor spreading took place in the overriding plate (Ishizuka et al., 2011a). The switch to fluxed melting of a harzburgitic (i.e., prior melt-depleted and refractory) mantle generating boninitic magma took place by 48 Ma, and the change to fluxed melting in a counterflowing mantle resulting in "normal" arc magmatism took place 7–8 m.y. after subduction initiation. Subduction initiation and subsequent magmatic evolution seem to have occurred nearly simultaneously along the length of the IBM subduction system.

Understanding magmatic evolution of the arc after subduction initiation has been significantly improved. However, characteristics of the overriding plate prior to subduction initiation, i.e., basement of the future IBM arc system, is still not well constrained. This hampers understanding of the tectonic setting leading to subduction initiation, and hence, the capacity to provide information needed to evaluate contrasting models of subduction initiation generally.

Seafloor drilling by IODP (International Ocean Discovery Program) Expedition 351 was conducted to recover rock samples formed in association with subduction initiation as well as the pre-inception basement of the IBM arc. It is particularly important to understand the age and origin of the arc basement to establish constraints on the tectonic situation at initiation, and reveal the duration and extent of seafloor spreading associated with subduction initiation.

In this contribution, we focus on the age of the present-day reararc basement as drilled in the Amami Sankaku Basin (ASB). We report $^{40}Ar/^{39}Ar$ ages of this basement as well as its major element composition. Based on this new dataset, the origin of the general arc basement crust, and the implications with respect to the tectonic setting at subduction initiation are discussed.

2. Geological background

The drill site of IODP Expedition 351, U1438, is located in the Amami Sankaku Basin now located in a reararc position relative to the Kyushu–Palau Ridge (KPR), and assumed reararc area of the proto-IBM arc (Fig. 1a, b). The KPR is a remnant arc separated from the IBM arc by arc rifting and backarc spreading after 25 Ma in the Shikoku and Parece-Vela Basins (Ishizuka et al., 2011b). The KPR was active in the Eocene and Oligocene (e.g., Mizuno et al., 1977; Ishizuka et al., 2011b). The extinct spreading centre of the West Philippine Basin (CBF rift) is truncated by the KPR at ~15°N (Fig. 1a). Radiometric ages for volcanic rocks collected from the northern to central KPR range in age between 43 and 25 Ma but are mostly between 27 and 25 Ma, indicating arc volcanism ended on the KPR at about this time (Ishizuka et al., 2011b). This observation has been reinforced by studies of the volcaniclastic deposits recovered at U1438 (Arculus et al., 2015; Brandl et al., 2017). The core record shows that the input of volcanic debris from the KPR ended abruptly around 25 Ma (Fig. 2), implying that arc rifting and opening of the Shikoku and Parece Vela Basins initiated at ~25 Ma (Ishizuka et al., 2011b). This interpretation is generally consistent with the estimated timing of rifting and spreading of the Shikoku Basin based on magnetic anomaly data and seafloor fabric observations. Okino et al. (1994) identified a magnetic lineation corresponding to Anomaly 7 in the westernmost (oldest) margin of the basin and suggested spreading started at 26 Ma. The lack of systematic age variations of volcanic rocks along the KPR indicates that rifting was initiated almost concurrently along the entire ridge between 30°N and 11°N.

Regarding the oldest volcanic record of the KPR, Brandl et al. (2017) reported on the geochemical compositions of glasses (occurring as inclusions in minerals) formed at the KPR from ~25 to 40 Ma at U1438. The sedimentary section containing the oldest volcaniclastic material above the igneous basement of U1438 was estimated to be between 40 and 57 Ma based on micropaleontological information (Fig. 2; Arculus et al., 2015). This is consistent with the oldest age of an andesitic rock recovered (43.29 Ma) and a 48.5 Ma granodiorite from Minami-Koho seamount at the intersection between the KPR and Daito Ridge (Fig. 3; Mizuno et al., 1977; Ishizuka et al., 2011b). However, direct and conclusive age data for the oldest volcanism on the KPR has not been previously obtained.

Crustal models based on wide-angle seismic profiles indicate that the KPR has a variable crustal thickness of 8–23 km (Nishizawa et al., 2016); the thicker parts of the ridge include an expanded middle crust section with Vp of 6.0–6.8 km/s, indicating a similar crustal structure to that observed beneath the IBM arc (e.g., Kodaira et al., 2007). In its reararc area, significant structural variation along the KPR is present, such as the ocean basins like the ASB and Kikai Basin (Fig. 1b), and remnant arcs preserved as the Daito Ridges, indicating a complex geologic and tectonic evolution in this region (Nishizawa et al., 2016) prior to subduction initiation to form the IBM arc.

The Daito Ridges region is a complex array of ridges and basins (Fig. 1a, b). The region comprises three remnant arcs: the Amami Plateau, the Daito and Oki-Daito Ridges, and two ocean basins between these ridges (the Kita-Daito and Minami-Daito Basins). Granitoids and arc-related volcanic rocks of Cretaceous age are exposed on the Amami Plateau (e.g., Hickey-Vargas, 2005) which has a crustal thickness of up to 19 km (Nishizawa et al., 2014). Geochemical characteristics of the volcanic rocks are consistent with formation of the Plateau by Cretaceous subduction zone magmatism (Hickey-Vargas, 2005). The Daito Ridge is generally east–west trending and intersects the KPR at its eastern end. Low-grade metamorphic rocks, sedimentary rocks, and some volcanic rocks were recovered by dredging, apparently from beneath Eocene sedimentary rocks (Mizuno et al., 1978). Recent shallow drilling using the Deep Sea Boring Machine System (BMS) recovered fresh volcanic rocks from the eastern part of the Daito Ridge. The recovered andesites, with distinctive trace element characteristics of arc magmas, yielded $^{40}Ar/^{39}Ar$ ages of 116.9 and 118.9 Ma (Ishizuka et al., 2011b). These ages are significantly older than any other volcanism in the IBM arc, and reinforce the crucial point that the Daito Ridge comprises Mesozoic arc rocks overlain by middle Eocene sedimentary rocks.

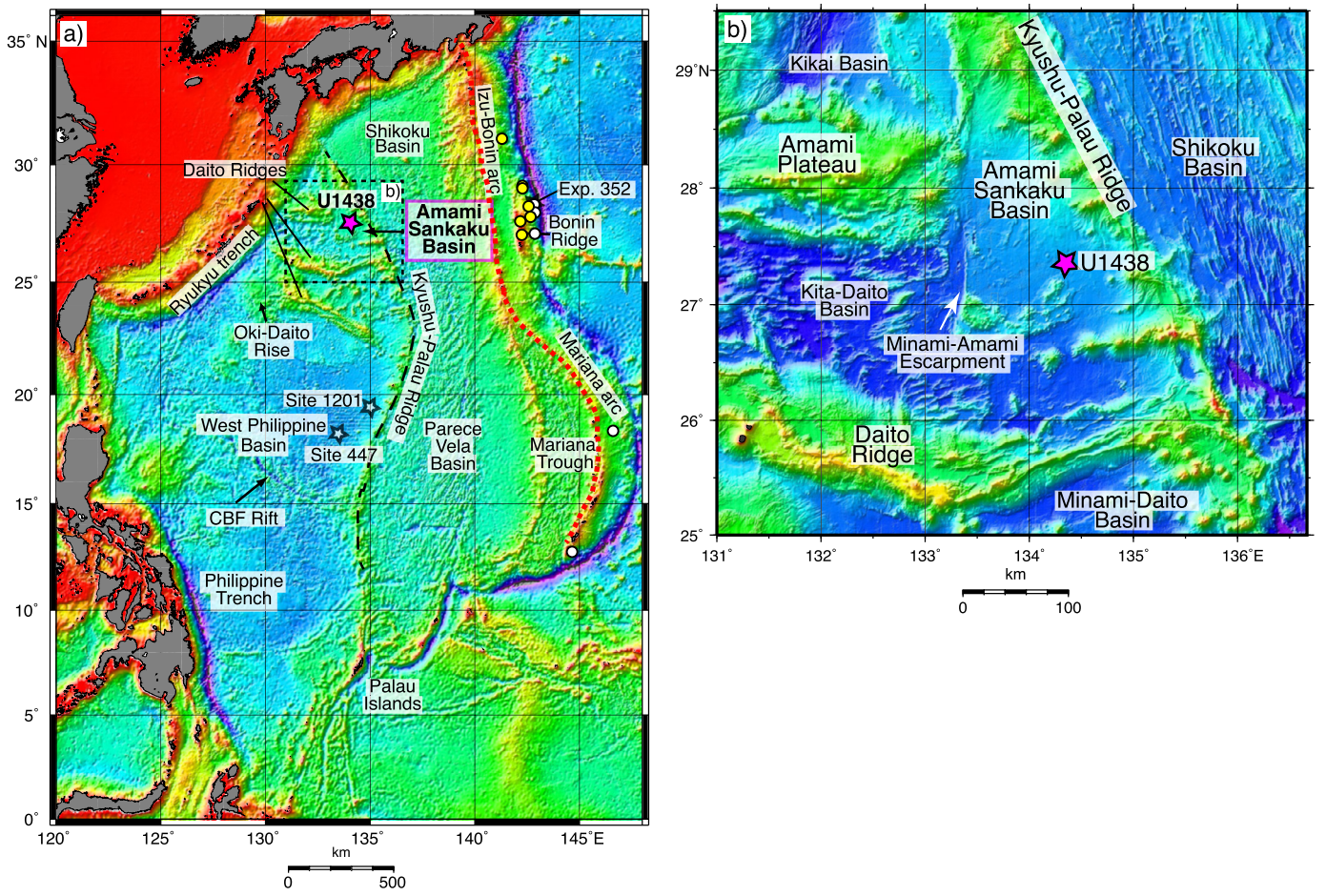

Fig. 1. a) Location map of drill site U1438 of IODP Exp. 351 in the Philippine Sea. The Izu–Bonin–Mariana (IBM) arc trench system forms the convergent boundary between the Pacific and Philippine Sea Plates. The localities of previously dated samples are also shown: white dots represent forearc basalts and yellow dots boninites (Cosca et al., 1998; Ishizuka et al., 2006, 2011a). b) Detailed bathymetric map of the drill site.

The Oki-Daito Ridge (Fig. 1a) is a WNW–ESE trending ridge characterised by crust ranging from 20 to 23 km in thickness (Nishizawa et al., 2014), and is regarded as another Mesozoic remnant arc (Tani et al., 2012). A large bathymetric high west of the Oki-Daito Ridge is the Oki-Daito Rise, which partially overlaps the western part of the Oki-Daito Ridge (Fig. 1a). The Rise is characterised by much thinner crust (10–15 km) compared to the Oki-Daito Ridge, and occurrence of basalts with Ocean-Island Basalt (OIB)-like geochemical characteristics with an age range between 40 and 44 Ma (Ishizuka et al., 2013).

Remnant arc terranes of the Daito Ridges region are separated by intervening seafloor of the Kita-Daito and Minami-Daito Basins (Fig. 1a, b). The Kita-Daito Basin, separating the Amami Plateau and the Daito Ridge, has a thin crust of 4 to 6 km based on seismic velocity structure (Nishizawa et al., 2014). Nishizawa et al. (2014) concluded this basin could have formed in a backarc setting. The Minami-Daito Basin, located between the Daito and Oki-Daito Ridges, has abundant bathymetric highs, and has a crust of 7–10 km thickness (Nishizawa et al., 2014). Basalts recovered from sills at Deep Sea Drilling Project (DSDP) Site 446 in the western part of the Basin and by shallow drilling at a seamount in the basin clearly have OIB-like geochemical characteristics (e.g., Hickey-Vargas et al., 2006; Ishizuka et al., 2013). These basalts have $^{40}Ar/^{39}Ar$ ages of 43 to 51 Ma. The age of formation of the Kita-Daito and Minami-Daito basins is currently not known.

The Amami Sankaku Basin is bordered to the west by a major N–S striking fault scarp (Minami-Amami Escarpment) and by the Amami Plateau, to the south by the Daito Ridge, and to the northeast by the KPR (Fig. 1b). Multichannel seismic reflection profiles across the ASB (Higuchi et al., 2007; Nishizawa et al., 2016) reveal a 1–2 km thick sedimentary section. The sediment is underlain by igneous basement with a thickness of around 5.5 km. Since the sedimentary sequence of this basin is isolated from any drilled sections in the Philippine Sea, no age constraints have previously been obtained for the formation of this Basin prior to drilling at Site U1438.

3. Drilled section and samples studied

Site U1438 of IODP Exp. 351 is located on flat-lying sediments at 4700 m water depth in the ASB (Fig. 1a, b). Igneous basement was reached after coring the entire sediment section. The cored interval comprises 5 units (Expedition 351 Scientists, 2015). The uppermost Unit I comprises hemipelagic sediment with intercalated ash layers, presumably sourced from explosive volcanism in the Ryukyu and Kyushu arcs. Units II and III host a series of volcaniclastic gravity-flow deposits, recording the magmatic history of the IBM arc between ~40 and 25 Ma (Fig. 2; Brandl et al., 2017). Unit III is characterised by coarse-grained volcaniclastic material compared to Unit II, and repetitive conglomerate- and sandstone-dominated intervals. Siliceous pelagic sediment (Unit IV) underlies Unit III with less coarse-grained sediment input. Unit IV is the most lithologically diverse, and characterised by the occurrence of reddish radiolaria-bearing mudstone, interbedded with layers of siltstone in the middle and lower parts. Basaltic andesite cobbles from the lower part of the unit have quench features, and all ap-

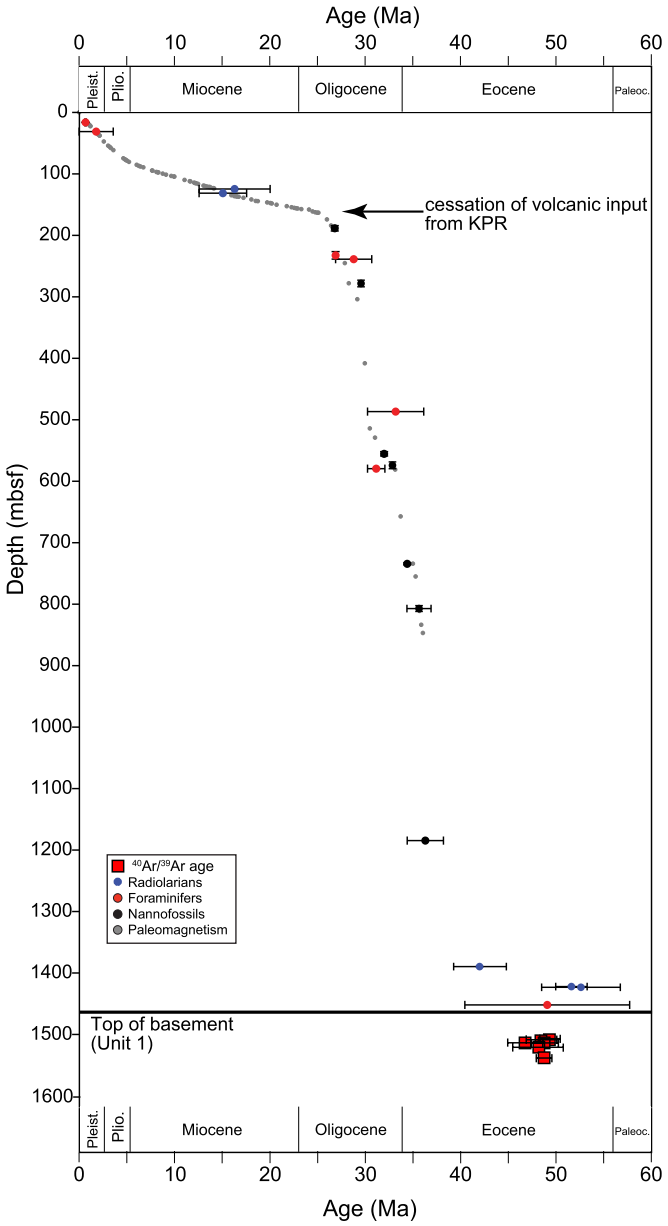

Fig. 2. Age–depth plot for Site U1438 based on biostratigraphic and palaeomagnetic data. ^{40}Ar/^{39}Ar ages obtained in this study are also shown with 2σ error.

pear concordant with the overlying and underlying sedimentary rocks. These features suggest that the basaltic andesites are shallow intrusive rocks, most likely sills.

Drilling at Site U1438 encountered oceanic basement. A basalt section, named as Unit 1, is dominantly composed of sheet lava flows. This unit continues to the bottom of the Hole at 1611 mbsf, and 44 m of core material was recovered in total. Numerous flow contacts were identified in Unit 1 including some with chilled margins, and this unit has been divided into 6 subunits (Fig. 4). Paleomagnetic measurements show consistent shallow plunges of maximum anisotropy axes, which implies these basalts were emplaced as sheet flows rather than pillow lavas (Expedition 351 Scientists, 2015).

Basalts have diverse but mainly microcrystalline to fine-grained textures. Phenocrysts are present in approximately half of the basalts and consist of plagioclase, clinopyroxene and spinel, together with olivine pseudomorphs. There is no obvious interval reflective of significant age gaps within Unit 1 except an occurrence of a piece of limestone at 1571 mbsf (Expedition 351 Scientists, 2015). For major element analysis, 98 samples were selected to reveal compositional variation along the entire section of Unit 1. Three samples of andesitic sills from Unit IV were also analysed.

Samples for age dating were selected exclusively based on freshness. Unit 1c is formed of relatively coarse-grained and holocrystalline basalts dominantly composed of plagioclase and clinopyroxene showing ophitic–subophitic textures, and contain minimal amounts of interstitial poorly-crystallised material. This makes Unit 1c the most suitable for dating; accordingly, all dated samples were selected from six different intervals within this Subunit.

4. Analytical procedures

4.1. Major element chemistry

About 20 g of rock chips were ultrasonically cleaned with distilled water, and then crushed by an iron pestle and pulverised using an agate mortar. Whole rock major elements were analysed on glass beads, prepared by fusing 1:10 mixtures of 0.5 g subsamples and lithium tetraborate. The glass beads were analysed using a Panalytical Axios XRF spectrometer at the Geological Survey of Japan/AIST. External error and accuracy are generally <2% (2.s.d), but Na could have as much as ~7% error. The data for each element are in agreement with accepted values of international standards within errors (Table S1).

4.2. $^{40}Ar/^{39}Ar$ dating

Ages of the basement samples from Site U1438 were determined using the ^{40}Ar/^{39}Ar dating facility at the Geological Survey of Japan/AIST. Details of the procedures are reported in Ishizuka et al. (2009). 20–25 mg of phenocryst-free groundmass, crushed and sieved to 186–250 μm in size, was analysed using a stepwise heating procedure. The samples were treated in 6N HCl for 30 minutes and then 4N HNO_3 for 30 minutes at 95 °C with stirring to remove any alteration products (clays and carbonates) present in interstitial spaces. After this treatment, samples were examined under a microscope, and microphenocrysts of clinopyroxene were removed. This procedure effectively separated and concentrated fresh plagioclase in the groundmass and microphenocrysts. Sample irradiation was done at the CLICIT facility of the Oregon State University TRIGA reactor for 4 h. Sanidine separated from the Fish Canyon Tuff (FC3) was used for the flux monitor and assigned an age of 27.5 Ma, which has been determined against our primary standard for our K–Ar laboratory, Sori biotite, whose age is 91.2 Ma (Uchiumi and Shibata, 1980).

A CO_2 laser heating system (NEWWAVE MIR10-30) was used at continuous wave mode for sample heating. A faceted lens was used to obtain a 3.2 mm-diameter beam with homogenous energy distribution to ensure uniform heating of the samples during stepwise heating analysis. Argon isotopes were measured on a IsotopX NGX noble gas mass spectrometer fitted with a Hamamatsu Photonics R4146 secondary electron multiplier in a peak-jumping mode.

Correction for interfering isotopes was achieved by analyses of CaF_2 and $KFeSiO_4$ glasses irradiated with the samples. The blank of the system including the mass spectrometer and the extraction line was 2.9×10^{-14} ml STP for ^{36}Ar, 1.4×10^{-13} ml STP for ^{37}Ar, 1.0×10^{-14} ml STP for ^{38}Ar, 1.2×10^{-14} ml STP for ^{39}Ar and 1.9×10^{-12} ml STP for ^{40}Ar. The blank analysis was done every 2 or 3 step analyses. All errors for ^{40}Ar/^{39}Ar results are reported at one standard deviation. Errors for ages include analytical uncer-

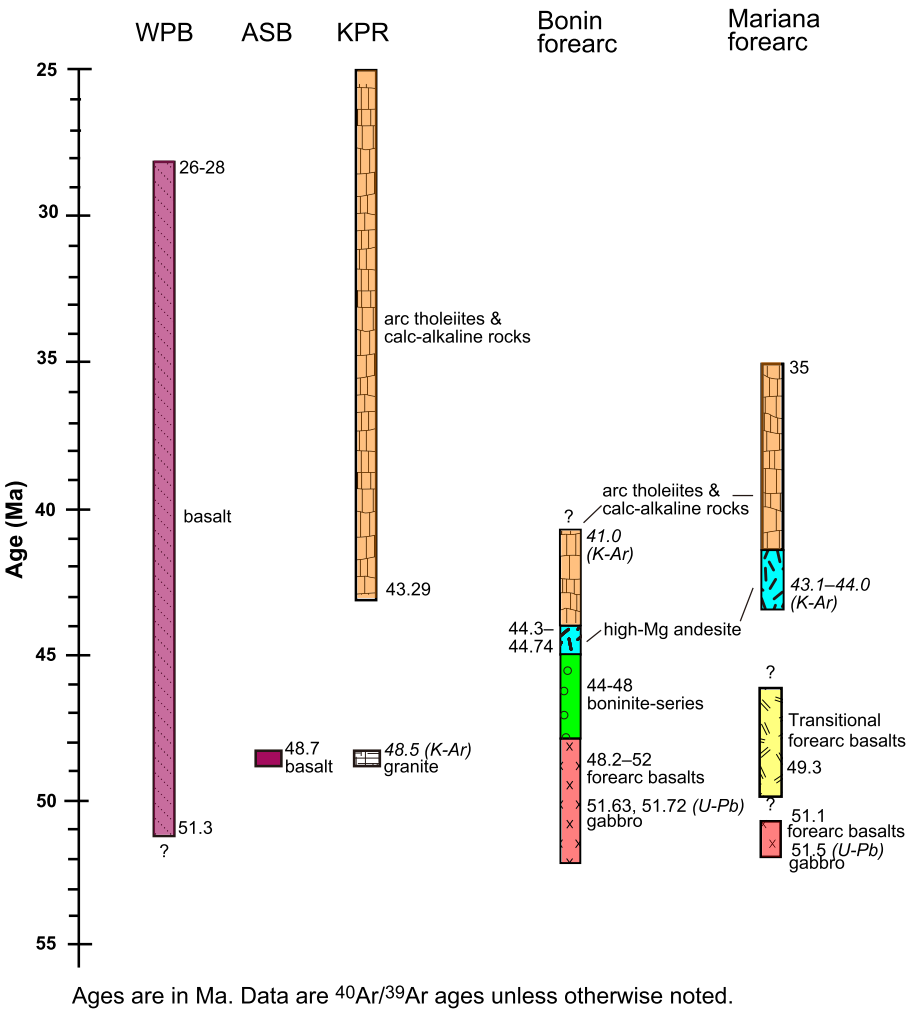

Fig. 3. Compilation of $^{40}Ar/^{39}Ar$, K–Ar, and U–Pb zircon dating results for igneous rocks from the IBM forearc, KPR, ASB and West Philippine Basin, modified after Ishizuka et al. (2014a). For data sources, see Ishizuka et al. (2011a, 2011b).

tainties for Ar isotope analysis, correction for interfering isotopes and J value estimation. An error of 0.5% was assigned to J values as a pooled estimate during the course of this study. Results of Ar isotopic analyses and correction factors for interfering isotopes are presented in supplementary data (Table S2).

Plateau ages were calculated as weighted means of ages of plateau-forming steps, where each age was weighted by the inverse of its variance. The age plateaus were determined following the definition by Fleck et al. (1977). Inverse isochrons were calculated using York's least-squares fit, which accommodates errors in both ratios and correlations of errors (York, 1969).

5. Results

5.1. Major element composition

All the analytical data are presented in supplementary Table S1. Major element compositions of Unit 1 basalts show discernible variations with depth: Titania content clearly indicates discontinuous variation with depth, which strongly implies the occurrence of distinct subunits within this basalt section (Fig. 4). FeO*/MgO, Na_2O, CaO and Al_2O_3 also have similar discontinuous variations, similar to that of TiO_2, even though the distinction among the subunits is not as clear as the case for TiO_2 (Fig. 4). Subunit boundaries estimated based on Ti content variation, which is not likely to be modified by the effect of alteration, are consistent with petrographic determination of subunits within the basaltic section (Fig. 4). Subunit 1a has a uniquely large variation with depth, i.e., FeO*/MgO, TiO_2, and CaO decrease upward, while Na_2O and SiO_2 increase (Fig. 4). Low FeO*/MgO compared with basalts in Subunits 1b–1f (Fig. 4) results from both higher MgO (9–14%) and lower FeO* (4.7–9.6%) (Table S1). Na_2O/CaO increases from 0.2 to 0.8 upward within this Subunit toward the sediment contact (Fig. 4).

Potash content of the basalt has a different behaviour than the oxides presented above (Fig. 4). Potash is consistently low in Subunit 1c, while it is highly variable in other subunits. Subunit 1a has a range from near 0 to ~1 wt.%. There is significant difference between Subunit 1c and 1d, and Subunit 1d to 1f again showing a large variation ranging from <0.1 to 1 wt.%. Each subunit, even though not in a systematic way, appears to have a distinct variation in terms of K_2O content. The origin of major and trace element variation in the subunits of Unit 1, including the impacts of alteration, is considered in detail in Hickey-Vargas et al. (submitted).

Based on their composition, the Unit 1 basalts are tholeiitic, defined collectively by sharply increasing FeO*/MgO with increasing SiO_2 (Fig. 5a). Subunit 1a, however, shows a distinct trend with relatively low and constant FeO*/MgO with increasing SiO_2, and Na_2O reaching values similar to those of Unit IV andesites (Figs. 4 and 5a). Titania contents have a similar range to that of forearc basalt from the IBM forearc, but are significantly lower than MORB (compared at a similar SiO_2 (Fig. 5b) or MgO (not shown)) or tholeiitic

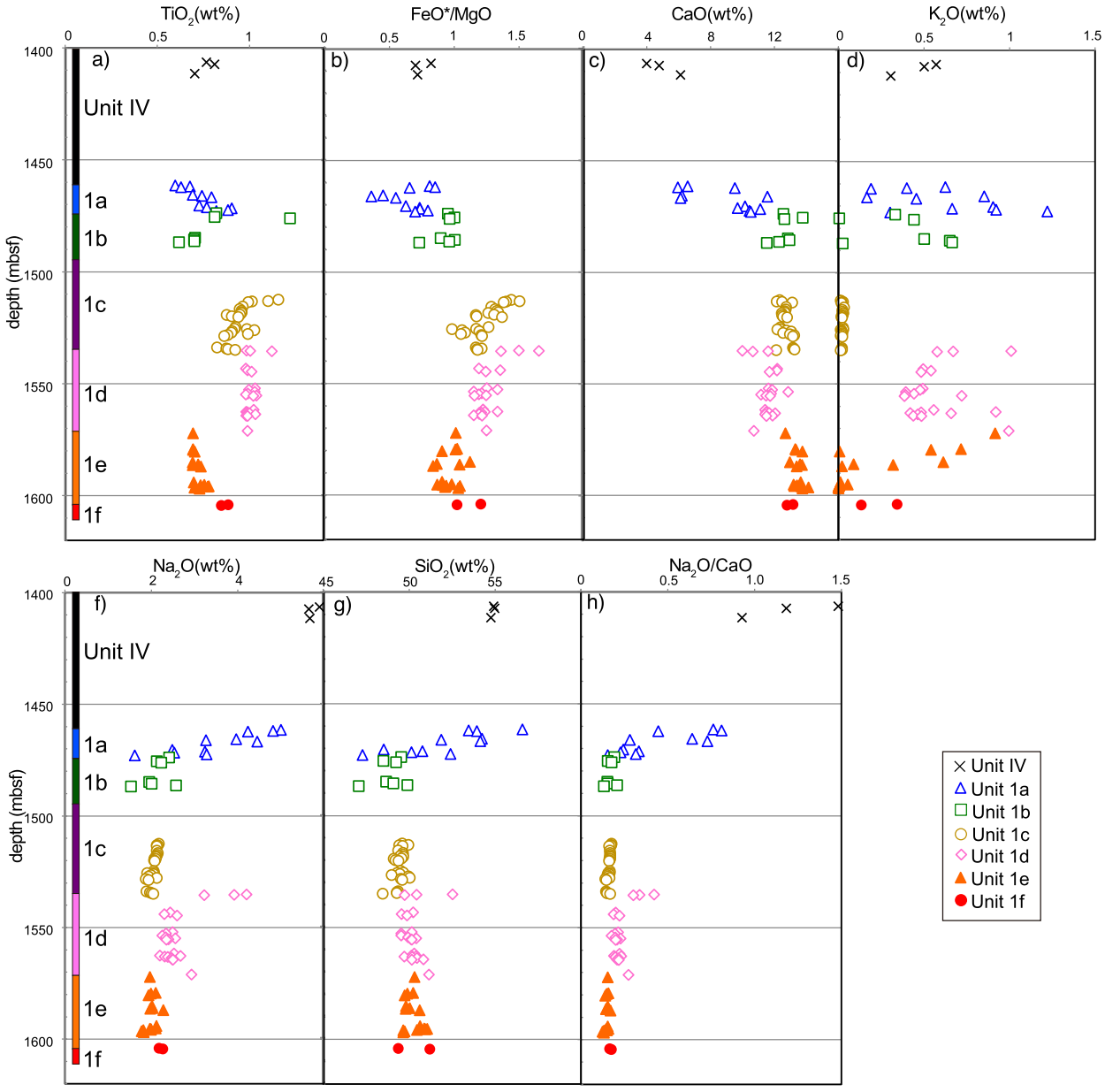

Fig. 4. Depth profiles of major element composition of Unit 1 basalts and Unit IV andesites from Site U1438.

basalts of the Philippine Sea backarc basin crust, with the exception of those from ODP Site 1201 and DSDP Site 447.

5.2. $^{40}Ar/^{39}Ar$ ages

Six samples from Unit 1 basalts (Site U1438) were dated by stepwise heating analysis (Table 1, S2; Fig. 6). These samples are from Subunit 1c, covering the core depth between 1509.1 mbsf and 1534.23 mbsf. All analyses for six samples gave well-defined age plateaus comprised of 86.1 to 100% of released gas. For each age spectrum, the inverse isochron age is identical to the weighted average age of plateau-forming steps, and the $^{40}Ar/^{36}Ar$ intercept of the inverse isochron is consistent with the atmospheric ratio within 2σ error. These data support the likelihood that the plateau ages are reliably recording the eruption ages of the basalt lavas. The plateau ages range from 46.8 to 49.3 Ma, all indistinguishable within 2σ error with a weighted average of $48.7 \pm 0.$ Ma. No systematic age variation is recognised with depth of the core (Fig. 2).

6. Discussion

6.1. Age of the Amami Sankaku Basin (ASB) igneous crust

$^{40}Ar/^{39}Ar$ dating reveals basalts from Subunit 1c of Site U1438 formed at around 48.7 Ma. Apart from the uppermost Subunit 1a, basalts from all Subunits of Unit 1 have very similar chemical characteristics with recognisable, yet small, differences among the Subunits. Combined with the lack of evidence for significant time gaps within the basalt lava section, it is reasonable to consider that at least the upper 150 m of the ASB igneous crust formed at around 48.7 Ma. Furthermore, these basalts are depleted low-K, low-Ti tholeiite (Figs. 4, 5), and dissimilar to the late stage alkaline and highly incompatible element-enriched basalts reported from other Philippine Sea backarc basins (e.g., Shikoku Basin: Ishizuka et al., 2009). This implies that the age of these basalts corresponds to that of the main stage of formation of the ASB igneous crust.

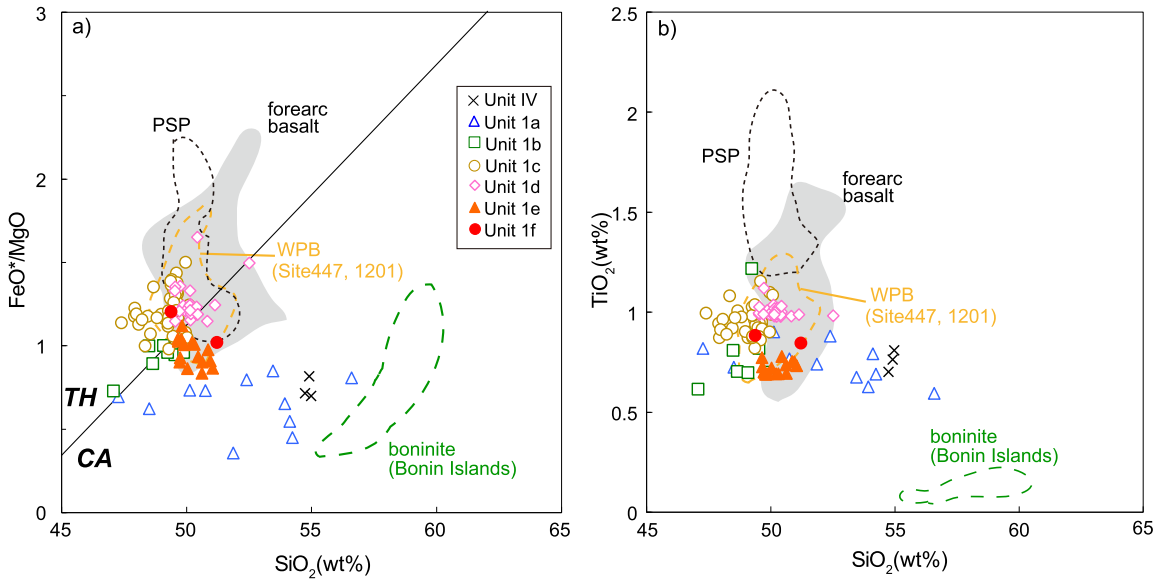

Fig. 5. Major element plots for the Unit 1 basalts from Site U1438. The line separating the tholeiitic and calc-alkaline field is from Miyashiro (1974). For data sources, see Ishizuka et al. (2014b).

Table 1
Results of stepwise-heating analyses of groundmass of basalts from Unit 1 of Site U1438.

Analysis No.	Sample No.	Steps	Total gas age ($\pm1\sigma$)	Plateau age ($\pm1\sigma$)				
			Integrated age (Ma)	Weighted average (Ma)	Inv. isochron age (Ma)	$^{40}Ar/^{36}Ar$ intercept	MSWD	Fraction of ^{39}Ar (%)
16029	1438E76R2 86-91	14	48.9 ± 0.6	**49.3 ± 0.5**	49.9 ± 0.8	289 ± 6	0.83	100.0
16023	1438E76R2 126-130	11	48.3 ± 0.9	**48.4 ± 0.8**	49.4 ± 2.4	278 ± 40	0.44	100.0
16026	1438E77R1 53-58	10	48.9 ± 1.0	**46.8 ± 0.9**	43.7 ± 2.1	331 ± 22	0.85	86.1
16010	1438E77R1 90-95	14	48.5 ± 0.8	**48.7 ± 0.7**	49.3 ± 1.0	291 ± 5	0.97	100.0
16027	1438E78R2 60-65	10	47.0 ± 1.6	**48.1 ± 1.3**	45 ± 4	332 ± 44	1.02	100.0
16024	1438E80R1 60-65	11	48.8 ± 0.5	**48.7 ± 0.4**	47.9 ± 0.7	303 ± 4	0.65	100.0

Inv. isochron age: inverse isochron age.
MSWD: mean square of weighted deviates ($(SUMS/(n-2))^{0.5}$) in York (1969).
Integrated ages were calculated using sum of the total gas released.
$\lambda_b = 4.962 \times 10^{-10}$ y^{-1}, $\lambda_e = 0.581 \times 10^{-10}$ y^{-1}, $^{40}K/K = 0.01167\%$ (Steiger and Jager, 1977).

The ages of these Unit 1 basalts are also consistent with the early or middle Eocene ages estimated for the overlying sedimentary rock section of Unit IV based on biostratigraphy (Fig. 2).

6.2. Spreading at subduction initiation

The ASB crust has been previously regarded as typical oceanic crust based on seismic data. Arculus et al. (2015) proposed that the ASB crust formed by seafloor spreading during the inception of the IBM subduction zone. This is mainly based on the geochemical similarity of the ASB basalt to forearc basalt, and the overlap of the biostratigraphically-constrained age and that of subduction initiation at the IBM arc. Direct dating of the basaltic flows pinpoints the age of formation of this crust. Our results confirm the formation of the ASB was contemporaneous with the 52–48 Ma magmatism of the forearc basalt reported from the IBM forearc (Fig. 3: Ishizuka et al., 2011a). In other words, the ASB crust is not pre-Eocene arc basement formed prior to subduction initiation and the development of the IBM arc.

In fact, the results indicate that the uppermost ASB crust formed about 3.3 m.y. after onset of forearc basalt magmatism (52 Ma). If we accept the model that subduction initiation and eruption of the earliest lavas of the IBM arc took place simultaneously along the entire length of the arc (Ishizuka et al., 2011a), these ages suggest that the oceanic igneous crust preserved at the rearc side of the future IBM arc formed later than that in the present-day forearc.

It is difficult to explain this situation as resulting from symmetric seafloor spreading, generating oceanic-type crust on which the chain of stratovolcanoes of the KPR was subsequently built. One possible explanation is that spreading following subduction initiation was affected by ridge jumps or migrations, and was asymmetric. Asymmetric spreading has been reported from mid-ocean ridges as well as from backarc basins (e.g., Allerton et al., 2000; Yamazaki et al., 2003; Deschamps and Fujiwara, 2003). Interaction of a spreading centre with a mantle plume or mantle wedge corner flow has been proposed as a cause of ridge migration (Müller et al., 2008; Martinez and Taylor, 2002). Asymmetric rheological and stress conditions due to the presence of subduction-related magmatism in an arc environment could also cause ridge migration (Martinez and Taylor, 2002; Deschamps and Fujiwara, 2003). Relative motion between the downgoing slab and overriding plate may also affect the location and rate of spreading (e.g., Martinez and Taylor, 2002; Sdrolias and Müller, 2006).

Asymmetric spreading accompanied by ridge migration observed in backarc basins could be analogous to spreading resulting from subduction initiation due to asymmetry of the newly developed plate boundary (e.g., Parson et al., 1990; Martinez and Taylor, 2002; Deschamps and Fujiwara, 2003; Brandl et al., 2017). It is known for example that at the earliest stages of backarc basin formation, spreading is unstable, possibly due to the interaction with the surrounding plates or regional tectonics (Parson et al., 1990; Yamazaki et al., 2003). These effects could also affect seafloor spreading during subduction initiation. Based on geological obser-

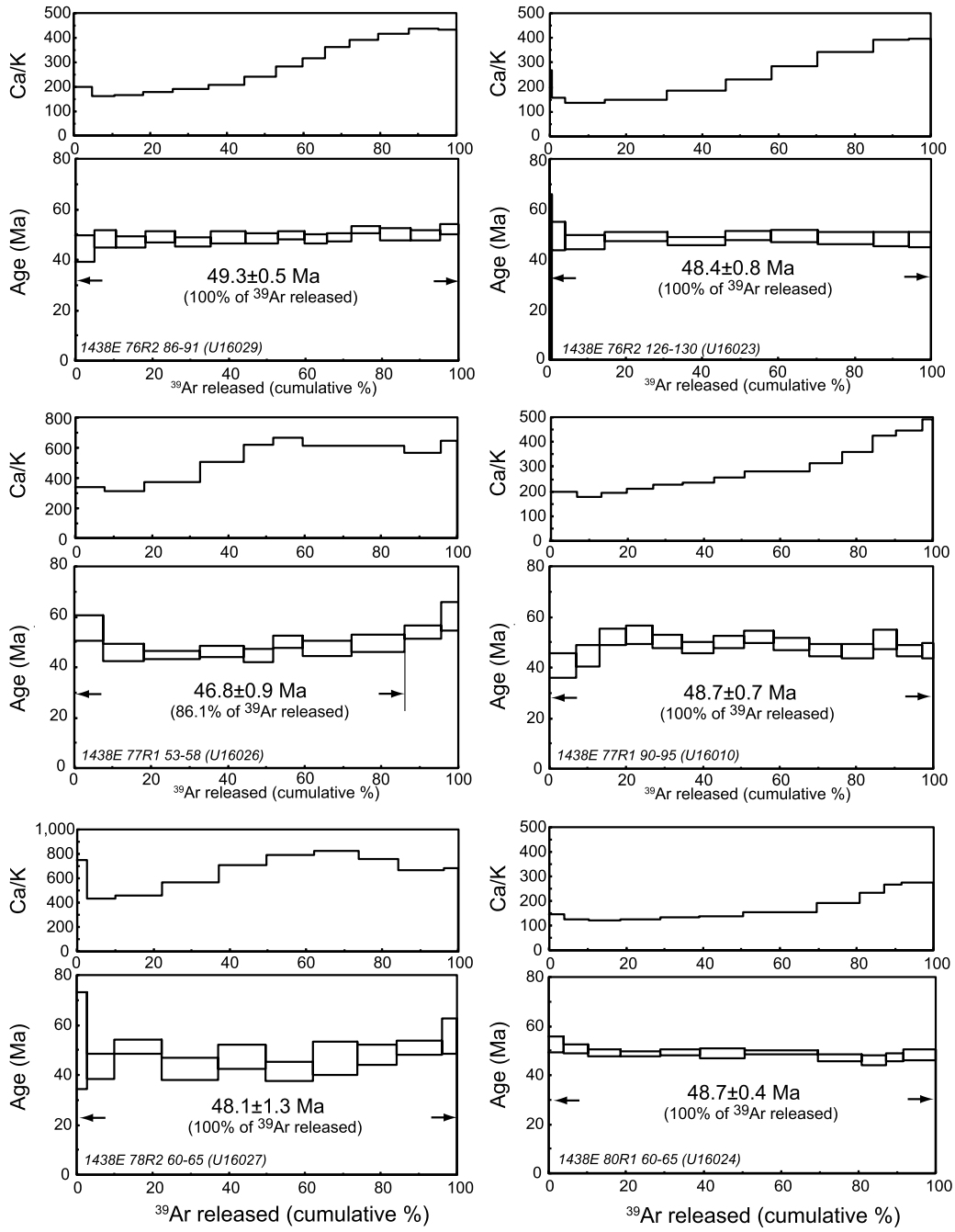

Fig. 6. $^{40}Ar/^{39}Ar$ age spectra and Ca/K plots for basalts from Unit 1 at Site 1438.

vations in the forearc area, the locus of the seafloor spreading (i.e., distribution of forearc basalt) and early arc magmatism were spatially and temporally juxtaposed (Ishizuka et al., 2011a; Reagan et al., 2013, 2017). Noting the ages of the ASB crust, the youngest forearc basalt and the oldest boninite almost overlap (Fig. 3), it seems possible that developing arc magmatism affected the mode of seafloor spreading. It has been noted that the locus of early arc magmatism migrated away from trench, i.e., migrated westward in the current geographic location during the first 7–8 m.y. after subduction initiation (Ishizuka et al., 2006, 2011a). Recent drilling of IODP Exp. 352 also confirmed that forearc basalt volcanism occurred closer to the trench than boninitic volcanism, and that they are fully transitional in composition (Fig. 1a, Reagan et al., 2017). On the other hand, no boninite has been recovered from KPR and volcaniclastic deposits cored at U1438. The volcanic record preserved at U1438 and the age of volcanics recovered from the KPR are no older than 48 Ma (Fig. 3: Ishizuka et al., 2011b; Brandl et al., 2017). These observations imply that volcanism within the rearc initiated up to several million years after volcanism in the frontal arc side. We conclude migration and instability of the locus of magmatism in the overriding plate developed during subduction initiation. The spreading axis might have moved away from the trench, i.e., ridge migration away from the trench and asymmetric spreading took place, which could be the reason that the ASB crust is younger than the oldest forearc basalt from the IBM forearc (Fig. 7).

Up to now, we have had minimal data for constraining the extent and rate of spreading in an overriding plate associated with subduction initiation. If the ASB crust formed through seafloor spreading following the onset of subduction, some estimates about

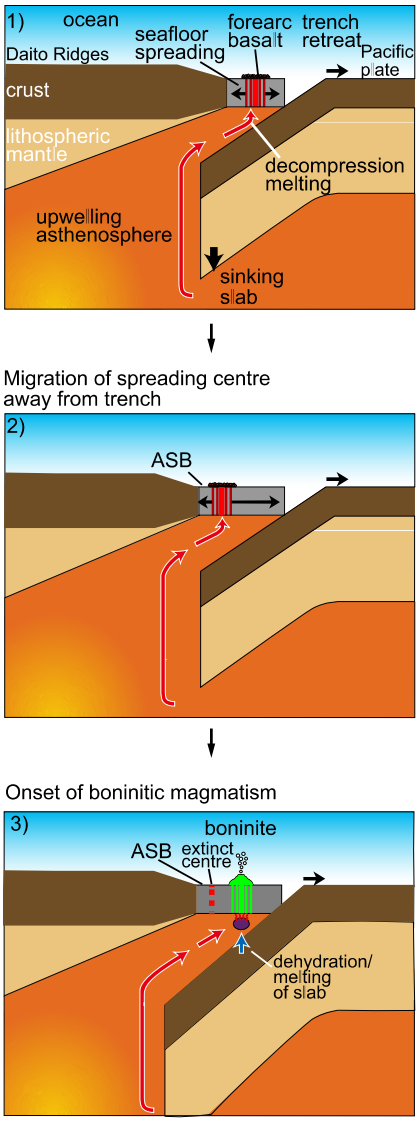

Fig. 7. Schematic cartoon illustrating the evolution of the proto-IBM arc including formation of the ASB following subduction initiation. ASB formed from a migrating spreading centre associated with subduction initiation.

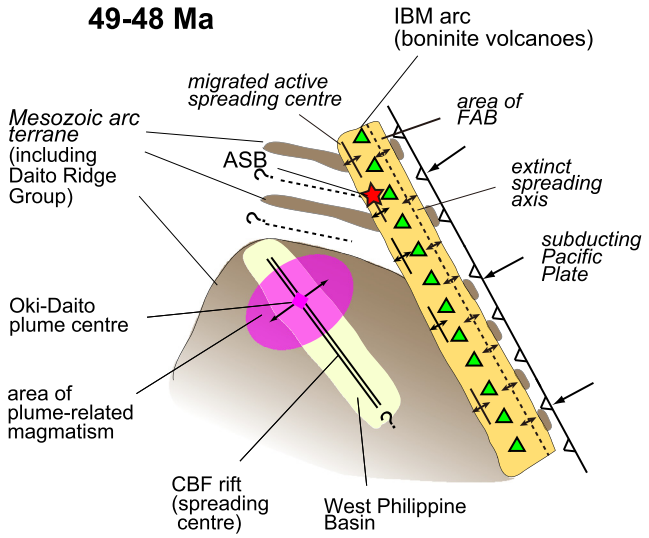

Fig. 8. Schematic diagram showing a tectonic reconstruction of the Philippine Sea Plate around 49–48 Ma. Seafloor spreading associated with subduction initiation formed ocean crust on the overriding plate mainly composed of Mesozoic arc terrane with intervening ocean basins. Boninite volcanoes and later island arc volcanoes formed on this ocean crust. Spreading of the West Philippine Basin commenced by this period, almost contemporaneously with onset of magmatism caused by arrival of Oki-Daito plume.

the mode of spreading can be made. The maximum we estimate for the width of the seafloor created by spreading associated with subduction initiation approaches 300 km, comprising the forearc slope, the modern and remnant arc sections and the ASB. If we assume a period of spreading of 3.3 m.y. (between 52 and 48.7 Ma), a full spreading rate is estimated to be 9.1 cm/yr, which corresponds to an intermediate-rate spreading centre, and is comparable to that of the West Philippine Basin (Deschamps and Lallemand, 2002; Ishizuka et al., 2013). In case of asymmetric spreading, however, the half spreading rate must have been faster (up to 15 cm/yr) than this estimate, and corresponds to fast spreading.

6.3. Implication to tectonics at subduction initiation

It is now clear that the ASB is not part of the Mesozoic remnant arc terrane of the Daito Ridges (Fig. 8). At the onset of subduction that created the proto-IBM arc, this terrane is supposed to have been on the overriding plate, and then rifted prior to the onset of spreading (Figs. 7, 8). In fact, pieces of Mesozoic crust have been reported along the forearc of the IBM arc. These include Cretaceous granitic bodies (Tani et al., 2012) and Jurassic basalt with Indian Ocean MORB character (Ishizuka et al., 2011a) in the Izu–Bonin section of the arc, and Mesozoic plutonic rocks from the Palau Trench (Malyarenko and Lelikov, 1995). The recovered plutonic rocks could be part of arc crust, and Jurassic basalt could correspond to intervening ocean basins among the arc massifs (e.g., Daito Ridge, Oki-Daito Ridge) of the Daito Ridges. These Mesozoic crustal rocks could be rifted blocks caused by onset of spreading on the overriding plate at subduction initiation, i.e., they provide supporting evidence for the model assuming that the overriding plate at subduction initiation was a Mesozoic arc terrane along the entire length of the future IBM arc (Fig. 8).

We conclude the overriding plate is not ocean crust as previously has been assumed (e.g., Stern and Bloomer, 1992; Stern, 2004; Ishizuka et al., 2006). Numerical and conceptual models for subduction initiation predict that the density contrast of juxtaposing plates plays an important role in triggering the sinking of the downgoing slab through gravitational instability (e.g., Matsumoto and Tomoda, 1983; Stern and Bloomer, 1992; Gurnis et al., 2004). Remnant arcs of the Daito Ridges have less dense and thicker crust relative to normal oceanic igneous crust, i.e., they are more buoyant (Nishizawa et al., 2014). Assuming the downgoing plate was the Pacific Plate, a tectonic setting wherein a plate composed of buoyant Mesozoic remnant arcs faced an oceanic plate is more favourable for subduction initiation than the situation where both plates consist of oceanic crust. Volcanoes of the IBM arc have been established on oceanic crust produced following the onset of subduction, but subduction began between juxtaposed oceanic crust (Pacific Plate) and remnant arc terranes (Daito Ridges).

Spreading of the West Philippine Basin is supposed to have initiated within the same Mesozoic terrane before 50 Ma, possibly almost contemporaneously with the onset of magmatism caused by arrival of Oki-Daito plume (Deschamps and Lallemand, 2002; Ishizuka et al., 2013). ODP Site 1201 (Fig. 1a) basalts cored from the northeastern margin of the West Philippine Basin, i.e., west of the KPR, share similar geochemical characteristics with the ASB basalts and FAB (e.g., Ti/V is lower, and more depleted in incompatible elements than N-MORB, Savov et al., 2006; Hickey-Vargas et al., 2006; Arculus et al., 2015). This strongly implies that a highly depleted MORB-type mantle source was present beneath

the Philippine Sea area during the period of subduction initiation, and appears to have been tapped during generation of both forearc basalt and basalts of the oldest part of the West Philippine Basin.

7. Conclusions

1) $^{40}Ar/^{39}Ar$ dating of the ASB provides the first radiometric age constraints on the arc basement in the rear side of the IBM arc. The age of final magmatism forming the oceanic igneous crust of the ASB is around 48.7 Ma. This age overlaps with the age range of forearc basalt from the IBM forearc, but is up to 3.3 m.y. younger than the onset of that forearc basalt activity, regarded as the marker for subduction initiation.

2) We conclude the combination of similarity in age range and geochemical character (e.g., low Ti/V, highly depleted in incompatible elements compared to N-MORB) implies the ocean crust of the ASB is equivalent to forearc basalt found in the IBM forearc. A corollary is ocean crust formed consequent to subduction initiation in the overriding plate extended from the forearc to reararc of the future IBM arc, i.e., the basement of the IBM arc is ocean crust formed at or soon after subduction initiation.

3) The age of the ASB ocean crust clearly indicates it is not part of the Mesozoic Daito Ridges. This Mesozoic terrane, which constituted the overriding plate at subduction initiation, had probably been rifted apart due to extension of the overriding plate during subduction initiation, and does not form the IBM arc basement. Where an overriding plate is composed of remnant arc terranes, it is more favourable for subduction initiation to be localised along the boundary between such terranes and oceanic lithosphere.

4) The temporal relationship between forearc basalt and ASB basalts seems to suggest that seafloor spreading during subduction initiation was strongly asymmetric as a result of ridge migration. With our estimated width (300 km) and minimum duration of spreading (3.3 m.y.), the spreading rate was intermediate to fast (9.1 to 15 cm/y) depending on the mode of spreading. Ridge migration might have been caused by unstable relative motion between the downgoing and overriding plates, emerging arc magmatism caused by onset of fluxed melting of mantle, and mantle wedge corner flow which was just being established after the slab started to sink.

Acknowledgements

This research used samples and data provided by the International Ocean Discovery Program. We thank the USIO staff and the SIEM Offshore crew for their invaluable assistance and skill during the Expedition. OI and YK appreciate JAMSTEC and J-DESC for their funding to join the expedition and post cruise research. IPS thanks UK-NERC for support for participation of the IODP cruise and part of the postcruise research. OI also used Grant-in-Aid (B) (No. 25287133) for shore-based research. We would like to thank K. Yamanobe for preparation of glass beads, A. Tokumoto for helping preparation of rock powder, and N. Geshi and Y. Ishizuka for the maintenance of GSJ XRF laboratory. The authors acknowledge the constructive reviews by an anonymous reviewer and helpful editorial comments by A. Yin.

Appendix A. Supplementary material

Supplementary material related to this article can be found online at https://doi.org/10.1016/j.epsl.2017.10.023.

References

Allerton, S., Escartin, J., Searle, R.C., 2000. Extremely asymmetric magmatic accretion of oceanic crust at the ends of slow-spreading segments. Geology 28, 179–182.

Arculus, R.J., Ishizuka, O., Bogus, K.A., Gurnis, M., Hickey-Vargas, R., Aljahdali, M.H., Bandini-Maeder, A.N., Barth, A.P., Brandl, P.A., Drab, L., do Monte Guerra, R., Hamada, M., Jiang, F., Kanayama, K., Kender, S., Kusano, Y., Li, H., Loudin, L.C., Maffione, M., Marsaglia, K.M., McCarthy, A., Meffre, S., Morris, A., Neuhaus, M., Savov, I.P., Sena, C., Tepley III, F.J., van der Land, C., Yogodzinski, G.M., Zhang, Z., 2015. A record of spontaneous subduction initiation in the Izu–Bonin–Mariana arc. Nat. Geosci. 8, 728–733. http://dx.doi.org/10.1038/NGEO2515.

Brandl, P., Hamada, M., Arculus, R.J., Johnson, K., Marsaglia, K.M., Savov, I.P., Ishizuka, O., Li, H., 2017. The arc arises: the links between volcanic output, arc evolution and melt composition. Earth Planet. Sci. Lett. 461, 73–84. http://dx.doi.org/10.1016/j.epsl.2016.12.027.

Brounce, M., Kelley, K.A., Cottrell, E., Reagan, M.K., 2015. Temporal evolution of mantle wedge oxygen fugacity during subduction initiation. Geology 43, 775–778.

Cosca, M.A., Arculus, R.J., Pearce, J.A., Mitchell, J.G., 1998. $^{40}Ar/^{39}Ar$ and K–Ar geochronological age constraints for the inception and early evolution of the Izu–Bonin–Mariana arc system. Isl. Arc 7, 579–595.

Deschamps, A., Fujiwara, T., 2003. Asymmetric accretion along the slow-spreading Mariana Ridge. Geochem. Geophys. Geosyst. 4 (10), 8622. http://dx.doi.org/10.1029/2003GC000537.

Deschamps, A., Lallemand, S., 2002. The West Philippine Basin: an Eocene to early Oligocene back arc basin opened between two opposed subduction zones. J. Geophys. Res. 107 (B12), 2322. http://dx.doi.org/10.1029/2001JB001706.

Expedition 351 Scientists, 2015. Izu–Bonin–Mariana Arc Origins: Continental Crust Formation at an Intra-oceanic Arc: Foundation, Inception, and Early Evolution. International Ocean Discovery Program, Preliminary Report, p. 351. https://doi.org/10.14379/iodp.pr.351.2015.

Fleck, R.J., Sutter, J.F., Elliot, D.H., 1977. Interpretation of discordant $^{40}Ar/^{39}Ar$ age-spectra of Mesozoic tholeiites from Antarctica. Geochim. Cosmochim. Acta 41, 15–32.

Gerya, T., 2011. Future directions in subduction modelling. J. Geodyn. 52, 344–378. http://dx.doi.org/10.1016/j.jog.2011.06.005.

Gurnis, M., Hall, L.C., Lavier, L., 2004. Evolving force balance during incipient subduction. Geochem. Geophys. Geosyst. 5, Q07001. http://dx.doi.org/10.1029/2003GC000681.

Hickey-Vargas, R., 2005. Basalt and tonalite from the Amami Plateau, northern West Philippine Basin: new Early Cretaceous ages and geochemical results, and their petrologic and tectonic implications. Isl. Arc 14, 653–665.

Hickey-Vargas, R., Savov, I.P., Bizimis, M., Ishii, T., Fujioka, K., 2006. Origin of diverse geochemical signatures in igneous rocks from the West Philippine Basin: implications for tectonic models. In: Christie, D.M., Fisher, C.R., Lee, S.-M., Givens, S. (Eds.), Back-Arc Spreading Systems: Geological, Biological, Chemical and Physical Interactions. In: AGU Geophys. Monogr., vol. 166. AGU, Washington, D.C., pp. 287–303.

Higuchi, Y., Yanagimoto, Y., Hoshi, K., Unou, S., Akiba, F., Tonoike, K., Koda, K., 2007. Cenozoic stratigraphy and sedimentation history of the northern Philippine Sea based on multichannel seismic reflection data. Isl. Arc 16, 374–393.

Ishizuka, O., Kimura, J., Li, Y., Stern, R., Reagan, M., Taylor, R., Ohara, Y., Bloomer, S., Ishii, T., Hargrove III, U., 2006. Early stages in the evolution of Izu–Bonin arc volcanism: new age, chemical, and isotopic constraints. Earth Planet. Sci. Lett. 250, 385–401. http://dx.doi.org/10.1016/j.epsl.2006.08.007.

Ishizuka, O., Yuasa, M., Taylor, R.N., Sakamoto, I., 2009. Two contrasting magmatic types coexist after the cessation of back-arc spreading. Chem. Geol. 266, 283–305.

Ishizuka, O., Tani, K., Reagan, M.K., Kanayama, K., Umino, S., Harigane, Y., Sakamoto, I., Miyajima, Y., Yuasa, M., Dunkley, D.J., 2011a. The timescales of subduction initiation and subsequent evolution of an oceanic island arc. Earth Planet. Sci. Lett. 306, 229–240. http://dx.doi.org/10.1016/j.epsl.2011.04.006.

Ishizuka, O., Taylor, R.N., Yuasa, M., Ohara, Y., 2011b. Making and breaking an island arc: a new perspective from the Oligocene Kyushu–Palau arc, Philippine Sea. Geochem. Geophys. Geosyst. 12, Q05005. http://dx.doi.org/10.1029/2010GC003440.

Ishizuka, O., Taylor, R.N., Ohara, Y., Yuasa, M., 2013. Upwelling, rifting and age-progressive magmatism from the Oki-Daito mantle plume. Geology 41, 1011–1014. http://dx.doi.org/10.1130/G34525.1.

Ishizuka, O., Tani, K., Reagan, M.K., 2014a. Izu–Bonin–Mariana fore-arc crust as a modern ophiolite analogue. Elements 10, 115–120. http://dx.doi.org/10.2113/gselements.10.2.115.

Ishizuka, O., Umino, S., Taylor, R.N., Kanayama, K., 2014b. Evidence for hydrothermal activity in the earliest stages of intraoceanic arc formation: implication to ophiolite-hosted hydrothermal activity. Econ. Geol. 109, 2159–2177.

Kodaira, S., Sato, T., Takahashi, N., Ito, A., Tamura, Y., Tatsumi, Y., Kaneda, Y., 2007. Seismological evidence for variable growth of crust along the Izu intraoceanic arc. J. Geophys. Res. 112, B05104. http://dx.doi.org/10.1029/2006JB004593.

Leng, W., Gurnis, M., 2015. Subduction initiation at relic arcs. Geophys. Res. Lett. 42, 7014–7021. http://dx.doi.org/10.1002/2015GL064985.

Maffione, M., Thieulot, C., van Hinsbergen, D.J.J., Morris, A., Plumper, O., Spakman, W., 2015. Dynamics of intraoceanic subduction initiation: 1. Oceanic detachment fault inversion and the formation of supra-subduction zone ophiolites. Geochem. Geophys. Geosyst. 16, 1753–1770. http://dx.doi.org/10.1002/2015GC005746.

Malyarenko, A.N., Lelikov, E.P., 1995. Granites and associated rocks in the Philippine Sea and the East China Sea. In: Tokuyama, H., Shcheka, S.A., Isezaki, N. (Eds.), Geology and Geophysics of the Philippine Sea. Terra Pub., Tokyo, pp. 311–328.

Martinez, F., Taylor, B., 2002. Mantle wedge control on back-arc crust accretion. Nature 416, 417–420.

Matsumoto, T., Tomoda, Y., 1983. Numerical-simulation of the initiation of subduction at the fracture-zone. J. Phys. Earth 31, 183–194.

McKenzie, D.P., 1977. The initiation of trenches: a finite amplitude instability. In: Talwani, M., Pitman III, W.C. (Eds.), Island Arcs, Deep Sea Trenches and Back-Arc Basins. In: Maurice Ewing Series, vol. 1. AGU, Washington, DC, pp. 57–61.

Miyashiro, A., 1974. Volcanic rock series in island arcs and active continental margins. Am. J. Sci. 257, 609–647.

Mizuno, A., Shibata, K., Uchiumi, S., Yuasa, M., Okuda, Y., Nohara, M., Kinoshita, Y., 1977. Granodiorite from the Minami-koho Seamount on the Kyushu–Palau Ridge, and its K–Ar age. Bull. Geol. Surv. Jpn. 28, 5–9.

Mizuno, A., Okuda, Y., Nagumo, S., Kagami, H., Nasu, N., 1978. Subsidence of the Daito Ridge and associated basins, North Philippine Sea. AAPG Mem. 29, 239–243.

Müller, R.D., Sdrolias, M., Gaina, C., Roest, W.R., 2008. Age, spreading rates, and spreading asymmetry of the world's ocean crust. Geochem. Geophys. Geosyst. 9, Q04006. http://dx.doi.org/10.1029/2007GC001743.

Nikolaeva, K., Gerya, T.V., Marques, F.O., 2010. Subduction initiation at passive margins: numerical modeling. J. Geophys. Res. 115, B03406. http://dx.doi.org/10.1029/2009JB006549.

Nishizawa, A., Kaneda, K., Katagiri, Y., Oikawa, M., 2014. Wide-angle refraction experiments in the Daito Ridges region at the northwestern end of the Philippine Sea plate. Earth Planets Space 66, 25. http://dx.doi.org/10.1186/1880-5981-66-25.

Nishizawa, A., Kaneda, K., Oikawa, M., 2016. Crust and uppermost mantle structure of the Kyushu–Palau Ridge, remnant arc on the Philippine Sea plate. Earth Planets Space 68, 30. http://dx.doi.org/10.1186/s40623-016-0407-3.

Okino, Y., Shimakawa, Y., Nagaoka, S., 1994. Evolution of the Shikoku Basin. J. Geomagn. Geoelectr. 46, 463–479.

Parson, L.M., Pearce, J.A., Murton, B.J., Hodkinson, R.A., Bloomer, S., Ernewein, M., Huggett, Q.J., Miller, S., Johnson, L., Rodda, P., Helu, S., 1990. Role of ridge jumps and ridge propagation in the tectonic evolution of the Lau back-arc basin, Southwest Pacific. Geology 18, 470–473.

Reagan, M.K., Hanan, B.B., Heizler, M.T., Hartman, B.S., Hickey-Vargas, R., 2008. Petrogenesis of volcanic rocks from Saipan and Rota, Mariana Islands, and implications for the evolution of nascent island arcs. J. Petrol. 49, 441–464.

Reagan, M.K., Ishizuka, O., Stern, R.J., Kelley, K.A., Ohara, Y., Blichert-Toft, J., Bloomer, S.H., Cash, J., Fryer, P., Hanan, B.B., Hickey-Vargas, R., Ishii, T., Kimura, J.I., Peate, D.W., Rowe, M.C., Woods, M., 2010. Fore-arc basalts and subduction initiation in the Izu–Bonin–Mariana system. Geochem. Geophys. Geosyst. 11, Q03X12. http://dx.doi.org/10.1029/2009GC002871.

Reagan, M.K., McClelland, W.C., Girard, G., Goff, K.R., Peate, D.W., Ohara, Y., Stern, R.J., 2013. The geology of the southern Mariana fore-arc crust: implications for the scale of Eocene volcanism in the western Pacific. Earth Planet. Sci. Lett. 380, 41–51.

Reagan, M.K., Pearce, J.A., Katerina Petronotis, K., et al., 2017. Subduction initiation and ophiolite crust: new insights from IODP drilling. Int. Geol. Rev.. http://dx.doi.org/10.1080/00206814.2016.1276482.

Savov, I.P., Hickey-Vargas, R., D'Antonio, M., Ryan, J.G., Spadea, P., 2006. Petrology and geochemistry of West Philippine Basin basalts and early Palau–Kyushu arc volcanic clasts from ODP Leg 195, Site 1201D: implications for the early history of the Izu–Bonin–Mariana Arc. J. Petrol. 47, 277–299.

Sdrolias, M., Müller, R.D., 2006. Controls on back-arc basin formation. Geochem. Geophys. Geosyst. 7, Q04016. http://dx.doi.org/10.1029/2005GC001090.

Steiger, R.H., Jäger, E., 1977. Subcommision on Geochronology: convention on the use of decay constants in geo- and cosmochronology. Earth Planet. Sci. Lett. 36, 359–362.

Stern, R.J., 2004. Subduction initiation: spontaneous and induced. Earth Planet. Sci. Lett. 226, 275–292.

Stern, R.J., Bloomer, S.H., 1992. Subduction zone infancy: examples from the Eocene Izu–Bonin–Mariana and Jurassic California Arcs. Geol. Soc. Am. Bull. 104, 1621–1636.

Tani, K., Ishizuka, O., Ueda, H., Shukuno, H., Hirahara, Y., Nichols, A.R.L., Dunkley, D.J., Horie, K., Ishikawa, A., Morishita, T., Tatsumi, Y., 2012. Izu–Bonin Arc: intra-oceanic from the beginning? Unraveling the crustal structure of the Mesozoic proto-Philippine Sea Plate. In: Abstract in AGU Fall Meeting 2012. AGU, Washington, D.C., United States.

Taylor, R.N., Nesbitt, R.W., Vidal, P., Harmon, R.S., Auvray, B., Croudace, I.W., 1994. Mineralogy, chemistry, and genesis of the Boninite Series Volcanics, Chichijima, Bonin Islands, Japan. J. Petrol. 35, 577–617.

Uchiumi, S., Shibata, K., 1980. Errors in K–Ar age determination. Bull. Geol. Surv. Jpn. 31, 267–273 (in Japanese with English abstract).

Yamazaki, T., Seama, N., Okino, K., Kitada, K., Joshima, M., Oda, H., Naka, J., 2003. Spreading process of the northern Mariana Trough: rifting-spreading transition at 22°N. Geochem. Geophys. Geosys. 4 (9), 1075. http://dx.doi.org/10.1029/2002GC000492.

York, D., 1969. Least squares fitting of a straight line with correlated errors. Earth Planet. Sci. Lett. 5, 320–324.